Stem Cell Research (2015) 15, 30–41

Available online at www.sciencedirect.com

ScienceDirect

www.elsevier.com/locate/scr

Impact of preconditioning with retinoic acid during early development on morphological and functional characteristics of human induced pluripotent stem cell-derived neurons

Sandra Horschitz[a], Friederike Matthäus[a], Anja Groß[a,1], Jan Rosner[a,b], Marta Galach[c,d], Wolfgang Greffrath[b], Rolf-Detlef Treede[b], Jochen Utikal[c,d], Patrick Schloss[a,*], Andreas Meyer-Lindenberg[a]

[a] *Department of Psychiatry and Psychotherapy, Central Institute of Mental Health, University of Heidelberg/Medical Faculty Mannheim, Germany*
[b] *Department of Neurophysiology, Center for Biomedicine and Medical Technology Mannheim, University of Heidelberg/Medical Faculty Mannheim, Mannheim, Germany*
[c] *Skin Cancer Unit, German Cancer Research Center (DKFZ), Heidelberg, Germany*
[d] *Department of Dermatology, Venereology and Allergology, University Medical Center Mannheim, University of Heidelberg/Medical Faculty Mannheim, Mannheim, Germany*

Received 23 October 2014; received in revised form 21 April 2015; accepted 30 April 2015
Available online 9 May 2015

Abstract
Human induced pluripotent stem cells (hiPSCs) are a suitable tool to study basic molecular and cellular mechanisms of neurodevelopment. The directed differentiation of hiPSCs via the generation of a self-renewable neuronal precursor cell line allows the standardization of defined differentiation protocols. Here, we have investigated whether preconditioning with retinoic acid during early neural induction impacts on morphological and functional characteristics of the neuronal culture after terminal differentiation. For this purpose we have analyzed neuronal and glial cell markers, neuronal outgrowth, soma size, depolarization-induced distal shifts of the axon initial segment as well as glutamate-evoked calcium influx. Retinoic acid preconditioning led to a higher yield of neurons vs. glia cells and longer axons than unconditioned controls. In contrast, glutamatergic activation and depolarization induced structural plasticity were unchanged. Our results show that the treatment of neuroectodermal cells with retinoic acid during early development, i.e. during the neurulation phase, increases the yield of neuronal phenotypes, but does not impact on the functionality of terminally differentiated neuronal cells.

* Corresponding author at: Biochemical Laboratory, Central Institute of Mental Health, J5, 68159 Mannheim, Germany. Fax: +49 621 1703 6255.
E-mail address: patrick.schloss@zi-mannheim.de (P. Schloss).
[1] Present address: Neurological Institute, University of Frankfurt, Frankfurt, Germany.

http://dx.doi.org/10.1016/j.scr.2015.04.007
1873-5061/

Introduction

The reprogramming of adult somatic cells by expression of a few defined transcription factors, such as Oct4, Sox2, Klf4 and c-Myc, was a milestone in stem cell research (Takahashi and Yamanaka, 2006). Several applications for the resulting human induced pluripotent stem cells (hiPSCs) have been used since then for the generation of specific cell types for transplantation or for drug testing in certain disease models as well as studying basic cellular mechanisms in vitro. Since biopsies from the human peripheral or central nervous systems are rarely done, one focus lies on the generation of human neuronal cells due to their potential to investigate cellular and molecular aspects of mental diseases in vitro and to develop new therapeutic approaches for these diseases. Various protocols for the differentiation of neuronal cells from hiPSCs have been established so far, using different methodologies to study cellular and functional aspects of the in vitro generated neurons. These methods include quantification of neurite length, soma size, synaptic connectivity, cell-type specification, and neuronal excitability, e.g. (Brennand et al., 2011; Falk et al., 2012; Kim et al., 2011; Prè et al., 2014; Shi et al., 2012). With respect to functionality, Grubb and Burrone presented a method to visualize activity-dependent neuronal plasticity by immunofluorescence (Grubb and Burrone, 2010). In rat hippocampal primary cultures chronic mild depolarization with KCl had been shown to induce a movement of the axon initial segment (AIS) from the cell soma. This shift of the AIS was only observed in excitatory neurons and was reversible upon omission of KCl in the medium. The changes in the AIS position correlated with increases in current thresholds for action potential spiking indicating that the observed effects rely on functional mechanisms.

For the reproducible neuronal differentiation of hiPSCs a desirable beneficial step is the establishment of a self-renewable neuronal precursor cell (NPC) line (Falk et al., 2012; Marchetto et al., 2010). Such NPCs can be expanded extensively and subsequently differentiated to a defined neuronal population. The process of terminal neuronal differentiation in vitro then lasts several weeks which reflects the time-scale of the neuronal maturation in vivo (Kim et al., 2014; McCormick and Prince, 1987). Here, gradients of morphogenetic molecules including the vitamin A metabolite retinoic acid (RA) are known to play pivotal roles for the developing central nervous system (Maden, 2001, 2007). In recent years the effect of retinoids on neuronal differentiation has also been studied in vitro. This includes studies on the generation of neurons from mouse embryonic stem cells (Bain et al., 1996; Bibel et al., 2004; Rochette-Egly, 2014) and from hiPSCs (Sartore et al., 2011; Shi et al., 2012; Verpelli et al., 2013). Furthermore, RA has also been used for the differentiation of the teratocarcinoma line NCCIT (Gasimli et al., 2013), the neuronal differentiation of the human SHSY5Y neuroblastoma cells (Påhlman et al., 1984) and of mononuclear cells from peripheral blood (Horschitz et al., 2010). Moreover, RA has been applied for the neural differentiation of P19 mouse pluripotent carcinoma cells (Chen and Reese, 2011). In the latter case differentiation could also be induced with the RA precursor retinol, although with 160 fold less efficiency.

In the present study we have analyzed the influence of RA treatment on early developing NPCs, i.e. during the neurulation phase. Starting from one hiPSC line we generated two NPC lines only one of which was treated with RA already during the neurulation phase, whereas in both lines addition of RA was omitted after generation of NPCs and during terminal differentiation. The resulting NPCs were then analyzed for the expression of typical marker proteins. In addition, a differential transcriptome expression analysis was performed in the two generated NPC lines. Next, we studied the impact of early RA treatment on morphological and functional features of the differentiated neurons. In summary, our findings show that treatment with RA during NPC development significantly promotes neuronal versus glial differentiation and hereby influences neurite length and soma size. With respect to functional aspects preconditioning with RA during early development did not affect activity-dependent movement of the AIS from the cell soma nor glutamate-evoked calcium transients.

Materials and methods

Human induced pluripotent stem cell culture and generation of neuronal precursor cell lines

The generation of the hiPSC line was performed according to the method of Maherali et al. (Maherali et al., 2008). Briefly, hiPSCs were derived from dermal fibroblasts of a healthy donor with an inducible polycistronic lentiviral reprogramming vector coding for the four reprogramming genes Oct4, Sox2, Klf4, and c-Myc (Somers et al., 2010) (Ethics Committee II of Heidelberg University approval no. 2009-350N-MA for hiPSC generation). Human iPSCs were cultured on hESC-qualified Matrigel (BD Biosciences) in defined mTeSR medium (Stemcell Technologies). Cells were split 1:6 every 5–7 days using 1 mg/mL dispase (Stemcell Technologies).

To initiate differentiation cells were resuspended in KO-DMEM/F12 medium supplemented with 1% N2 (both Invitrogen) after dispase treatment and triturated carefully to single cells, first, using a 5 ml-pipette, second, a 200 μL-pipette, and finally, a glass pasteur pipette. Embryoid bodies (EBs) were formed according to the method described by Ungrin et al. (Ungrin et al., 2008). Here, 10,000 cells per well were seeded in a V-bottom shaped 96well plate coated with Pluronic F-127 (Sigma) to prevent cell attachment. The plate was centrifuged at 200*g* for 5 min. The next day, aggregates were scraped with a wide bore 1000 μL-tip and transferred to a bacterial-grade Petri dish. During floating culture the KO-DMEM/F12 medium was supplemented with 1% N2, 50 ng/mL noggin (Stemgent), 500 nM dorsomorphin (Tocris), 1 μM SB431542 (Sigma). Here, one cell line was preconditioned with 1 μM retinoic acid (RA; Sigma); this line is termed NPC^{+RA} throughout the manuscript. A second, independent line did not receive RA treatment (NPC^{-RA}). After four days of floating culture, EBs were plated on Matrigel-coated 6well plates in the same medium. When EBs attached to the plate (after 1–3 days) medium was changed to DMEM/F12 GlutaMAX supplemented with 1% N2, 2% B27, 2 mM L-glutamine, 100 μM MEM nonessential amino acids (all Invitrogen) and 20 ng/mL bFGF (R&D Systems). Neural rosette structures became visible after 10–14 days. Rosettes were picked with a needle and replated on Matrigel-coated 6well plates in the same medium. The highly proliferating cells were passaged approximately every two days 1:4 in the beginning.

After 2–3 splittings a homogeneous culture of NPCs was achieved. NPCs were cultured on poly-L-ornithine (Sigma) coated plates from then on with a split ratio of 1:2 once a week. The cells can be cryo-preserved in mFreSR medium (Stemcell Technologies) and were kept in culture up to passage 20 until now.

Directed differentiation of NPCs

For terminal neuronal differentiation both NPC lines, NPC^{+RA} and NPC^{-RA}, respectively, were seeded on Matrigel-coated 6well plates with 1.5 * 10^5 cells/well in DMEM/F12 GlutaMAX with 1% N2, 2% B27, 2 mM L-glutamine, 100 μM MEM nonessential amino acids and 20 ng/mL bFGF. On the next day differentiation was induced by bFGF withdrawal in the same medium. Since no other growth factors were applied, cells developed a mainly glutamatergic phenotype by a default mechanism (Stern, 2001). Medium was changed every other day and the neuronal culture survived up to 100 days.

Immunofluorescence, neuronal growth measurements and quantifications

For immunofluorescence analyses cells were grown on Matrigel-coated glass cover slips. At certain time points cells were fixed in 4% paraformaldehyde for 15 min at room temperature, washed in PBS and permeabilized with 0.1% Triton X-100 and 0.1% Na-citrate in PBS for 3 min at 4 °C. Afterwards, cells were blocked for 1 h in blocking solution (0.1% gelatine, 10% horse serum in PBS) at room temperature. Primary antibodies were diluted in blocking solution and incubated with the cells for 45 min at room temperature (antibodies and dilutions are listed below) (Table 1). Secondary antibodies conjugated to Alexa fluorophores (Invitrogen) were diluted 1:1000 and incubated for 45 min at room temperature before mounting the cells with ProlongGold (Invitrogen).

For quantification experiments cells were stained with the nuclear dye TOTO-3 diluted 1:200 together with the secondary antibodies. Images were acquired on a Leica TCS SP5 confocal laser scanning microscope using either an ×20 or an ×63 oil planachromat lens (Leica Microsystems). All images were processed using ImageJ (NIH). Neurite tracings were performed with the ImageJ plugin NeuronJ. Statistical analysis was performed using GraphPad software.

Table 1 List of applied antibodies, the respective supplier, and experimental dilution.

Antibody target (source)	Supplier	Dilution
Oct3/4 (rat)	R&D Systems	1:100
Sox2 (gt)	Santa Cruz	1:200
Pax6 (rb)	Covance	1:200
Nestin (rb)	Abcam	1:500
Tau (gp)	Synaptic Systems	1:200
Map2a (ms)	Abcam	1:200
β-tubulin III (rb)	Synaptic Systems	1:200
vGlut1 (gp)	Synaptic Systems	1:500
GAD1 (rb)	Synaptic Systems	1:200
GFAP (ms)	Synaptic Systems	1:500
AnkG (ms)	Neuromab	1:100

Flow cytometry

Cells were trypsinized and resuspended in culture medium. For each trial 5*10^5 cells were centrifuged and resuspended in FACS staining buffer (Becton Dickinson) and incubated for 20 min with APC-labelled anti-CD133 (1:10; Miltenyi Biotech) at room temperature. Cells were washed twice and measured with a Becton Dickinson FACS Calibur cytometer. 10,000 events were acquired per measurement and analyzed using the CellQuest Pro software. Isotype controls were taken from each cell line using APC-labelled mouse IgG1 antibody (AbD Serotec).

Transcriptional analysis

Total RNA was isolated with Trizol (Invitrogen) from NPC^{-RA} and NPC^{+RA} lines. A differential gene expression analysis was performed by GATC Biotech (InView Transcriptome Explore; GATC Biotech). Gene expression was analyzed using the Bowtie, TopHat, Cufflinks, Cuffmerge, Cuffdiff software suite.

Calcium imaging

For calcium imaging experiments NPCs were differentiated on Matrigel-coated 35 mm μ-dishes (Ibidi) with 2 * 10^5 cells/dish. First experiments were performed after 50 days of terminal differentiation. Cells were transferred into extracellular solution (Tyrode's solution) containing NaCl 137.6 mM, KCl 5.4 mM, $MgCl_2$ 0.5 mM, $CaCl_2$ 1.8 mM, glucose 5 mM and HEPES 10 mM (Roth), and were loaded with 3 μM FURA-2 AM (Calbiochem) and same amount (in μL) of Pluronic F-127 (Calbiochem) for 45–60 min at room temperature protected from light. Cells were washed twice with extracellular solution and mounted on the stage of an inverted microscope (Olympus IX81 equipped with cellR Imagingsystem). During the experiments cells were superfused with Tyrode's solution (1–3 mL/min) at room temperature. After alternating excitation with light of 340 nm and 380 nm wavelength, the ratio of the fluorescence emission intensities at 510 nm (340 nm/380 nm [510 nm]) was calculated and digitized at 1 Hz by an ORCA-R2 camera (Hamamatsu Photonics). This fluorescence ratio is a relative measurement of intracellular calcium concentration (Grynkiewicz et al., 1985). Regions of interest were drawn around cells which could easily be distinguished from adjacent cells. Relative changes in intracellular calcium were calculated by dividing the peak values by the initial baseline. An increase of >23% in response to 100 μM glutamate was considered significant (Greffrath et al., 2001), and only these cells were used for subsequent analyses. Normalization of calcium transients was performed by setting the maximum responses seen in an independent culture to 100% and adjusting all others accordingly.

Data analysis

Statistical analysis for neurite length measurements was performed with GraphPad Prism 3.0 in terms of One-way ANOVA followed by post-hoc Tukey's multiple comparison

tests. Soma size measurements were analyzed by unpaired t-test. The chosen level of significance was $p < 0.01$.

Results

Retinoic acid impacts on axonal growth of hiPSC-derived neuronal cultures

For the reproducible induction of hiPSC-derived neuronal cell cultures we aimed to generate self-renewable NPC lines since this method has the advantage to make the hiPSC culture dispensable once the NPC stadium is achieved. HiPSC and NPC lines were generated as described in the Materials and methods section (2.1 and 2.2). In the phase of neural induction NPC generation was performed in the absence and presence of RA during floating culture which resulted in the generation of two NPC lines, termed NPC^{-RA} and NPC^{+RA}. Both NPC lines were used between passage #10–20 for all here described experimental work. Cellular states were monitored during NPC generation and the two NPC lines were analyzed for the expression of neuronal precursor proteins Pax6, Nestin and Sox2 by immunofluorescence as well as for CD133/PROMININ (Uchida et al., 2000) by FACS (Fig. 1). No differences were observed between NPC^{-RA} and NPC^{+RA} in these analyses.

NPCs were cultured in the presence of bFGF and a simple withdrawal of the growth factor induced a terminal differentiation into mainly glutamatergic neurons. For a morphological comparison between NPC^{-RA} and NPC^{+RA} we monitored neuronal growth by measuring neurite lengths and soma sizes (Fig. 2). At certain time points differentiating cells were fixed and the length of the axons were determined after performing an immunofluorescent staining against the axonal protein tau. Accordingly, the length of the dendrites was measured after staining for the somatodendritic marker protein MAP2a. Here we found a remarkable difference between NPC^{-RA} and NPC^{+RA}: As shown in Fig. 2B, the length of the axons of NPC^{+RA}-derived neurons was significantly longer compared to NPC^{-RA}-derived neurons. This was observed already at day 5 of terminal differentiation whereas no significant differences were seen with respect to the dendrite length of the two cell lines over a differentiation period of 4 weeks. Regarding the soma size both cell lines showed a dramatic shrinkage in the beginning of differentiation until day 8, whereas no significant differences between NPC^{-RA} and NPC^{+RA} were observable.

Early retinoic acid treatment impacts on the cellular phenotype of differentiating neurons

Next, we compared the composition of the cell culture with respect to cellular phenotypes at certain time points during the first 51 days of differentiation. Immunofluorescence analyses were performed for the neuronal marker proteins

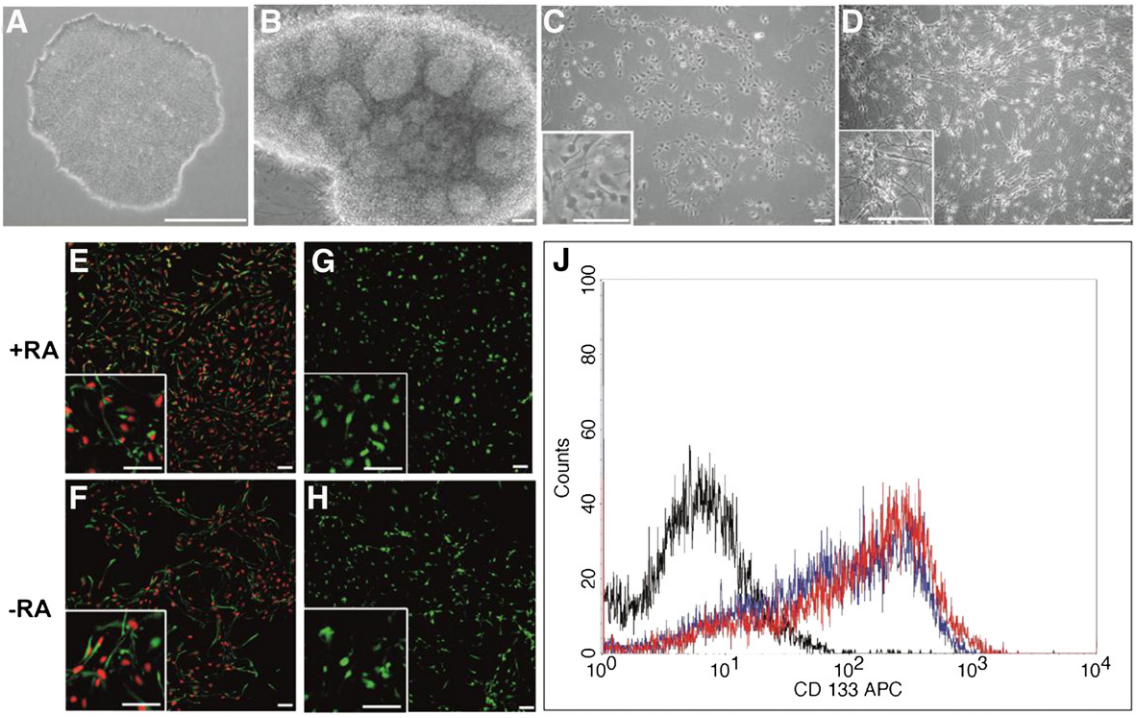

Figure 1 RA does not alter cellular states during differentiation of hiPSCs to NPCs. (A) A representative colony of hiPSCs growing on Matrigel. (B) Arising neural rosettes 7 days after plating of EBs on Matrigel. (C) A monolayer of NPCs after two further splittings of replated rosettes (picture of NPC^{+RA}). (D) Neuronal networks in differentiating NPCs (NPC^{+RA}) at day 53 after growth factor withdrawal. (E, F) Staining of Sox2 (red) and the neural precursor protein Nestin (green) in NPC^{+RA} and in NPC^{-RA}. (G, H) Staining of the neural precursor protein Pax6 in NPC^{+RA} and in NPC^{-RA}. Left lower squares in (C) to (H) show a section of cells in higher magnification. All stainings were performed at least three times ($n > 3$). (J) A representative FACS analysis of the neural-specific cell surface protein CD133/PROMININ is shown for both established NPC lines (NPC^{-RA}, red, and NPC^{+RA}, blue); ($n = 2$). The black line corresponds to the secondary antibody isotype negative control. Scale bar in inset (C) 10 μm, all other scale bars 50 μm.

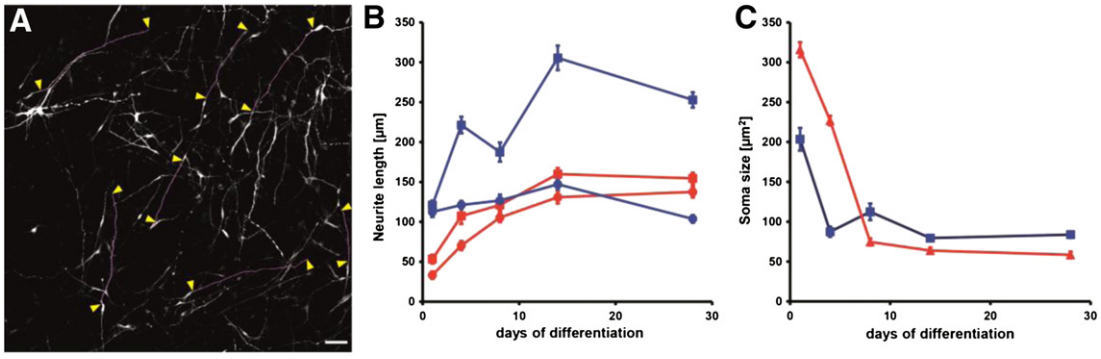

Figure 2 Early RA treatment during NPC generation promotes axonal outgrowth. Differentiating cells were stained at the indicated time points for the axonal marker protein tau and the somatodendritic marker protein MAP2a. The neurite lengths and soma sizes were determined with the plugin NeuronJ of the ImageJ software. A representative picture with appropriate tracings for MAP2a stained neurons of the NPC^{+RA} line on day 14 of differentiation is shown in (A). Yellow arrows point to beginning and ending of respective neurites. Scale bar 200 µm. The graphs show in (B) the lengths of dendrites (●,●) and axons (□,□) of NPC^{-RA}, red, and NPC^{+RA}, blue, respectively. For NPC^{+RA} axons were significantly longer than dendrites whereas no significant difference was observed for NPC^{-RA} (one-way Anova; $p < 0.01$). In (C) the shrinkage of the somas of the corresponding cell lines (NPC^{-RA}, red, NPC^{+RA}, blue) until day 28 of differentiation is shown. No significant differences between the two cell lines were observed (unpaired t-test; $p > 0.05$). At least 50 cells were measured per graph point. The graphs show results obtained from one representative differentiation; the whole experiment was performed three times with NPC^{+RA} and twice with NPC^{-RA} with similar results.

β-tubulin III, tau and MAP2a, and for the glial marker protein GFAP in order to determine the proportion of neuronal and glial cells. In addition, stainings for the cell type specific proteins vGlut1 and the GABA synthesizing protein GAD1 were performed. In all immunofluorescences the nuclear cell dye TOTO-3 was applied to enable quantifications. Typical immunofluorescence stainings are shown in Fig. 3C, where, however, the TOTO-3 staining is omitted for a better visualization of the cell type specific markers. In the quantification experiments the amount of MAP2a-positive cells and tau-positive cells were comparable to the amount of β-tubulin III-positive cells. Therefore in Fig. 3A only the results for β-tubulin III quantification are given as neuronal cell marker. In Fig. 3A it is shown that for both NPC lines the proportion of neuronal cells decreased during terminal differentiation while the proportion of glial cells rose. Importantly, at day 51 of differentiation neural cultures derived from NPC^{-RA} consisted of 23 ± 7% neurons and 75 ± 3% glial cells, whereas cultures derived from NPC^{+RA} consisted of 42 ± 5% neurons and 53 ± 11% glial cells. In both NPC lines the proportion of glutamatergic and GABAergic neurons rose within the neuronal subpopulation during terminal differentiation (Fig. 3B). At day 51 up to 80% glutamatergic neurons were determined for the NPC^{-RA} line and up to 90% glutamatergic neurons for the NPC^{+RA} line. GABAergic neurons were detectable in both lines, but with a distinct proportion only at day 51 of differentiation in both NPC lines (Fig. 3B).

Differential gene expression analysis of NPC^{-RA} and NPC^{+RA} lines

A comparative transcriptome analysis of NPC^{-RA} and NPC^{+RA} lines revealed RA-induced up-regulation of many neuronal genes as well as of several transcription factors. An exemplary overview of a selection of significantly up-regulated genes which are involved in neurodevelopment or neuronal differentiation is presented in Table 2. Detailed information of the total gene expression analysis is found under Supplementary data.

Early retinoic acid treatment does not influence AIS movement in glutamatergic neurons

The axon initial segment (AIS) is a specialized region in neurons where the action potential is initiated. It is located near the axon hillock and it comprises several AIS specific proteins, including AnkyrinG (AnkG), which is used here for an immunofluorescent localization of the AIS region. It was shown by Grubb and Burrone (2010) that chronic mild depolarization of glutamatergic neurons from rat hippocampal cultures induced a distal shift of the AIS. This movement was reversible and was not observed in GABAergic neurons (Grubb and Burrone, 2010). Here, neuronal cultures were depolarized by cultivation in neuronal differentiation medium containing 15 mM K^+ for two days at 37 °C with 5% CO_2. Control cultures were kept under the same conditions but without KCl addition. Afterwards, the cells were either fixed with 4% PFA or further cultivated for another two days in normal neuronal differentiation medium for recovery experiments and fixed thereafter. Immunofluorescent analyses were performed at day 50 of terminal differentiation for AnkG and the glutamatergic marker vGlut1 or the GABAergic marker GAD1, respectively. As shown in Fig. 4, mild chronic KCl treatment induced a significant distal AIS shift from the cell somata only in glutamatergic, but not in GABAergic neurons. This shift did not significantly differ between NPC^{-RA} and NPC^{+RA}-derived neurons (17.91 ± 1.07 µm and 13.03 ± 1.13 µm, respectively) and was reversible in both cell lines. At least 40 cells were analyzed per graph point.

Early retinoic acid treatment does not influence neuronal excitability by glutamate

Microfluorimetric measurements of free intracellular calcium were performed using the calcium dye FURA-2-AM in neuronal cultures after day 50 of terminal differentiation (n = 3 for NPC^{-RA} and NPC^{+RA}, each). Application of glutamate (100 μM) induced a significant rise (>23%) in intracellular calcium in about half of all cells of NPC^{+RA} under investigation (45.2 ± 24.4%; Fig. 5, left column); for NPC^{-RA} the responder rate was nominally lower (15.3 ± 6.1%). However, due to large variation seen between cultures (responder rates from 4.2 to 94%) this difference did not reach statistical significance. Glutamate evoked calcium transients displayed concentration dependence, the EC_{50} values were 16.6 μM and 19.1 μM (Hill slopes 0.63 ± 0.18 and 0.57 ± 0.13), respectively, and did not differ between treatments ($\log_{10} EC_{50} = -4.78 \pm 0.26$ and -4.72 ± 0.17; $p > 0.30$, student's t-test; Fig. 5C). Glutamate-induced Ca^{2+} influxes were completely blocked by 10 μM CNQX but not affected by 20 μM APV (data not shown).

Discussion

All-trans retinoic acid (RA), a metabolic compound derived from vitamin A, is well-known to play a pivotal role during the developing nervous system by activating nuclear receptors which are ligand-inducible transcription factors. In vivo RA contributes to patterning of the neural plate and neural tube in a concentration-dependent manner (Hansen et al., 2011; Maden, 2007) and it is required for cortical neurodevelopment (Siegenthaler et al., 2009). During in vivo brain development RA induces the differentiation of glia and other cells by activation of the transcription of many genes encoding transcription factors, enzymes, structural proteins as well as RA-inducible repressor genes (Maden, 2001).

Also in vitro RA has been shown to have a time- and concentration-dependent effect on neurodevelopment (Tonge and Andrews, 2010) and to induce different neuronal phenotypes from embryonic stem cells. In recent years most RA-related studies have been performed with mouse ES cells (Bain et al., 1996; Bibel et al., 2004; Rochette-Egly, 2014). Compared to human ES or iPS cells these cells often show differences in their neuronal in vitro cultures, especially regarding culture conditions or the time-scale of their neurodevelopment. In this line RA alone can induce the differentiation of glutamatergic neurons, together with sonic hedgehog (SHH) the differentiation of cholinergic and dopaminergic neurons, and together with ciliary neurotrophic factor (CNTF) the differentiation of dopaminergic neurons from mouse embryonic stem cells (for review see (Maden, 2007)). With respect to neuronal differentiation of hiPSCs it was demonstrated recently that the generation of glutamatergic neurons depends on the presence of RA (Zeng et al., 2010), and that the presence of RA is absolutely crucial for the development of cortical neurons with marker expression of all cortical layers (Shi et al., 2012). When comparing the literature for the impact of RA on neuronal differentiation from hiPSCs it is noticeable that there is a high diversity in i) the applied RA concentrations, ii) in the starting time point of application and iii) in the duration of the treatment during neuronal differentiation (Brennand et al., 2011; Chambers et al., 2009b; Falk et al., 2012; Marchetto et al., 2010; Shi et al., 2012; Tonge and Andrews, 2010). With this respect, several protocols for neuronal differentiation of human stem cells including iPSCs, have been reported (for overview see (Kim et al., 2014)). Based on a protocol of Zhang and colleagues (Zhang et al., 2001) neural commitment of ES cells or hiPSCs often starts with the formation and culturing of EBs for a short period of time. Then the EBs are grown in adherent culture in defined media containing N2 and B27 supplements and bFGF until the formation of "neural rosettes." These are then manually isolated and replated in Matrigel-coated plates until a homogeneous culture of NPCs is achieved which can be finally differentiated to neurons, astrocytes and oligodendrocytes both in vitro and in vivo (Zhang et al., 2001). Here, bioactive RA is known to exert caudalizing effects during CNS development in vivo and during neural differentiation of stem cells in vitro (Allodi and Hedlund, 2014; Liu and Zhang, 2011). For example, continuous addition of 1 μM RA to NPCs from day 3 of differentiation favoured the final differentiation to motor neurons (Lippmann et al., 2014). In another approach Amoroso and colleagues have added RA from day 5 after EB formation consequently for 31 days which resulted in efficient motor neuron differentiation (Amoroso et al., 2013).

At this point it is worthwhile mentioning, that the B27 supplement can be purchased containing 0.3 μM retinyl acetate which is a biologically inactive storage form of vitamin A. However, only dietary retinol bound to the retinol binding protein 4 (RBP4) is taken up into cells where it can then be stored either as retinyl esters or oxidized in two steps to the bioactive metabolite RA (Chen and Reese, 2011; Napoli, 2012; Orsolits et al., 2013). Interestingly, only some cell types seem to have the ability to take up retinol/RBP4 and to metabolize retinol to RA inside the cell. Newer data suggest that RA synthesized in one cell type can act on adjacent cells. This paracrine signalling is a common theme in development and the differentiation of cells in vitro (Gudas and Wagner, 2011).

In the present study we aimed to analyze the effect of early retinoid signalling already during the neural induction phase on the development of the neuronal culture. Therefore, two NPC lines were generated (NPC^{-RA} and NPC^{+RA}) one of which was treated with RA during the initial neural induction phase of EB formation (NPC^{+RA}). Thereafter both lines were treated equally, i.e. in the absence of biologically active RA in the culture medium. In the early phase of differentiation no difference in number or size of formed EBs was observed and also the onset of rosette formation was comparable. Both NPC lines were morphologically similar and did not differ within the expression of neural precursor marker proteins such as Pax6, nestin or Sox2, indicating that RA treatment during the neurulation phase did not influence NPC properties so far. A comparative transcriptome analysis of the two cell lines revealed a RA-induced expression of the transcription factor FoxG1 which is required for early telencephalon patterning (Hebert and Fishell, 2008) and, on the other hand, also of HoxA1 which is involved in hindbrain patterning (Chambers et al., 2009a). These findings suggest that early RA treatment induces a more general neuronal commitment of the NPCs whereas RA activity is needed also during later phases of development for hindbrain/spinal cord differentiation. To elucidate these interactions in more detail, a gene expression analysis of terminally differentiated neurons in the absence

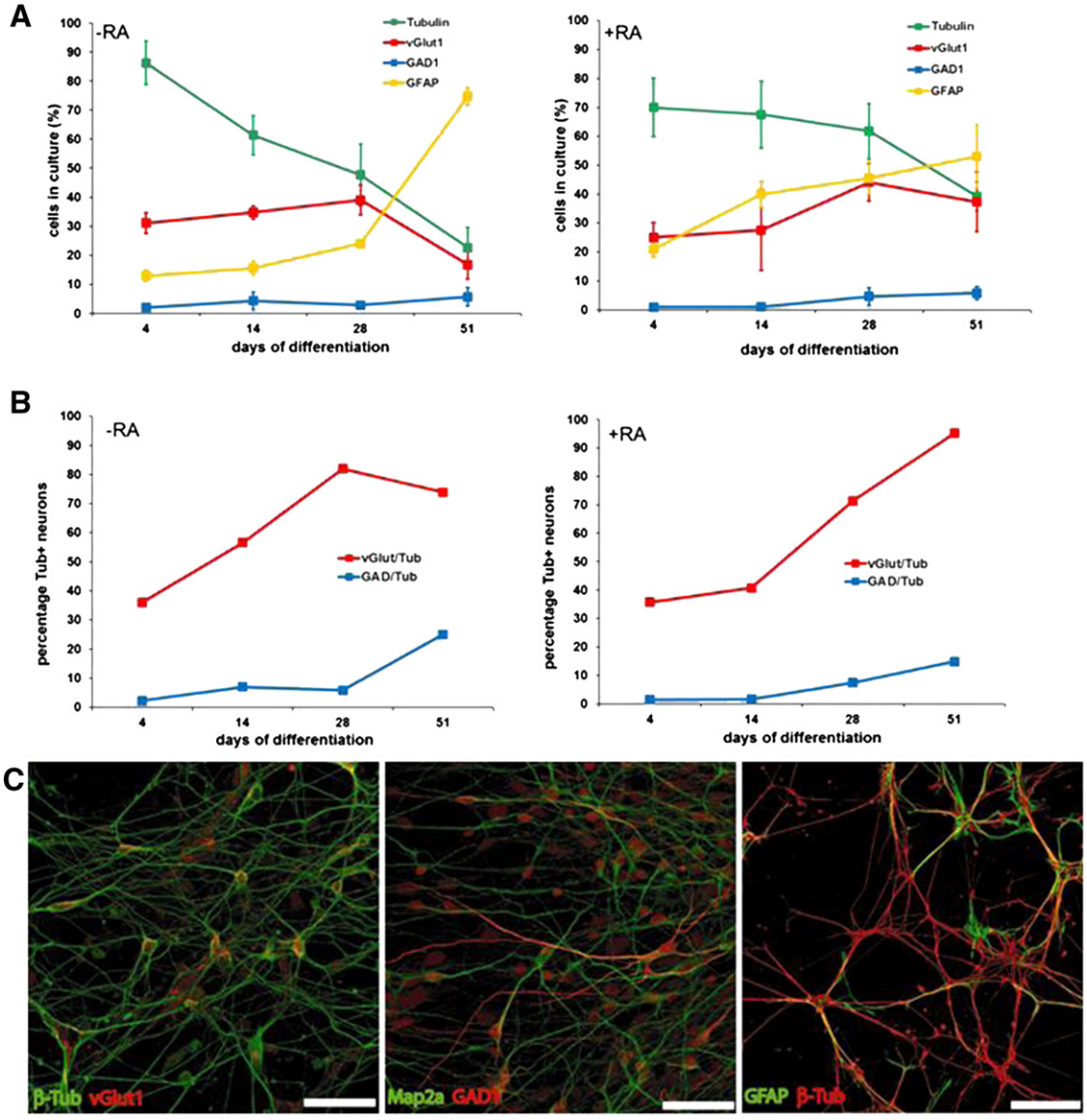

Figure 3 Early RA treatment influences cellular composition of differentiating neurons. (A) Specific marker proteins were stained by immunofluorescence at defined time points during differentiation together with the cell nuclear stain TOTO-3 and quantified using the ImageJ software. At least 50 cells were analyzed per staining and time point from at least three individual differentiations per cell line. In both NPC lines, NPC^{-RA} and NPC^{+RA}, the proportion of neuronal cells (β-tubulin-positive cells, green lines) decreased until day 51 of differentiation while the proportion of glial cells (GFAP-positive cells, yellow lines) rose accordingly. This effect is observed in the NPC^{-RA} line to a higher extent: at day 51 the culture consisted of 23 ± 7% neuronal cells (green line, left graph) and 75 ± 3% glial cells (yellow line, left graph) compared to 42 ± 5% neuronal cells (green line, right graph) and 53 ± 11% glial cells (yellow line, right graph) in the NPC^{+RA} line. In both cell lines the percentage of GABAergic cells (GAD1-positive, blue lines) is low during differentiation while the amount of glutamatergic cells steadily rises in RA-treated cells (red line). (B) Within the neuronal population (quantifications in relation to β-tubulin-positive cells) the percentage of glutamatergic cells (vGlut1-positive cells, red lines) increased to >80% for NPC^{-RA} (left graph) and to >90% for NPC^{+RA} (right graph) during differentiation. The amount of GABAergic cells (GAD1-positive, blue lines) was quite low in both cell lines and rose within the neuronal population up to 20% for NPC^{-RA} and up to 15% for NPC^{+RA} at day 51. In (C) representative stainings are shown for β-tubulin and vGlut1 (left), for MAP2a and GAD1 (middle), and for GFAP and β-tubulin (right). All displayed stainings were performed with NPC^{+RA}-derived neurons at different time points of terminal differentiation: d26 (β-tubulin + vGlut1), d51 (MAP2a + GAD1), d33 (GFAP + β-tubulin). Scale bars 50 μm.

versus presence of RA would be needed. In this regard, Paschaki and colleagues have performed a comparative transcriptome analysis of anterior and posterior tissues of murine embryos lacking the endogenous RA synthesizing enzyme retinaldehyde dehydrogenase 2 (Paschaki et al., 2013). These studies conducted at early stages of embryonic development revealed a down-regulation of the anterior FoxG1 as well as of the posterior HoxA1 in the RA-deficient mice.

Table 2 Selection of significantly up-regulated genes in NPC^{+RA} which are functional in neurodevelopment and differentiation.

Symbol	Name	Function	Expression rate	
			NPC^{-RA}	NPC^{+RA}
CNTN2	Contactin 2 (axonal)	Contributes to the organization of axonal domains	0.507	813.788
GRIK3	Glutamate receptor, ionotropic, kainate 3	Ligand-gated ion channel which plays an important role in excitatory synaptic transmission	330.134	700.422
SYT6	Synaptotagmin VI	Involved in Ca(2+)-dependent exocytosis of secretory vesicles	0.199	181.408
GAD2	Glutamate decarboxylase 2	Catalyzes the production of GABA	0	171.966
GFRA1	GDNF family receptor α1	Plays key role in the control of neuron survival and differentiation	0.656	110.978
SLC17A8	Vesicular glutamate transporter	Transports glutamate into synaptic vesicles	0	278.886
TBX3	T-box transcription factor 3	Transcriptional repressor and is thought to play a role in the anterior/posterior axis of the tetrapod forelimb	0	317.788
FOXG1	Forkhead box protein G1	Regulation of transcription; may play a role in brain development	0	270.053
NRXN3	Neurexin-3-alpha	Cell adhesion molecule involved in synaptic plasticity	0	201.342
HOXB3	Homeobox protein B3	Regulation of transcription	0	359.795
CACNA1A	Cav2.1 P/Q voltage-dependent calcium channel	Mediates the entry of calcium ions into excitable cells	0	620.947
DLX1	Homeobox protein DLX1	Transcriptional regulator of signals from multiple TGF-β superfamily members; may play a role in differentiation and survival of inhibitory neurons in the forebrain	0	246.376
SLC32A1	Vesicular inhibitory amino acid transporter	GABA and glycine uptake into synaptic vesicles	0	280.714
TM4SF1	Transmembrane 4 L6 family member 1	Mediates signal transduction events that play a role in the regulation of cell development, activation, growth and motility	0	501.596
SST	Somatostatin	Regulates the endocrine system and affects neurotransmission and cell proliferation	0	730.345
TFAP2B	Transcription factor AP-2β	Stimulates cell proliferation and suppresses terminal differentiation	0	172.863
HOXA1	Homeobox protein A1	Regulation of transcription	0	534.145
HOXA3	Homeobox protein A3	Regulation of transcription	0	368.739
HOXA7	Homeobox protein A7	Regulation of transcription	0	109.836
NPTX2	Neuronal pentraxin II	Involved in excitatory synapse formation	382.262	505.677
STMN2	Stathmin-2	Functions in microtubule dynamics and signal transduction; plays a regulatory role in neuronal growth	179.557	782.711

Expression rates are given in fragment per kilobase per million mapped reads (FPKM). Threshold for significance is the false discovery rate (FDR) adjusted p-value of test statistic for log2 (fold change) analyzed with Cuffdiff software (<5%).

In the transcriptome analysis of our NPC lines, the expression of several neuronal transcripts including various proteins involved in synaptic transmission was significantly up-regulated in the NPC^{+RA} sample. Interestingly, these included GABAergic genes, such as the vesicular GABA transporter and glutamic acid decarboxylase 2, as well as transcripts involved in glutamatergic neurotransmission like the vesicular glutamate transporter vGLUT3. Glia-specific transcripts, however, were not up-regulated in the NPC^{+RA} samples again suggesting that early RA treatment favours neuronal versus glial differentiation.

In order to investigate properties of terminally differentiated neurons we analyzed morphological aspects and the cellular composition of the NPC-derived cultures. Interestingly, the quantification of neuronal outgrowth revealed that early RA treatment promotes axonal growth which led to the development of neurons with axons twice as long as the dendrites. This corresponds to Dotti's model of a functional neuron (Dotti et al., 1988) and was only found in differentiated neurons of the NPC^{+RA} line. In addition, after 50 days of terminal differentiation neural cultures derived from NPC^{+RA} contained significantly more neurons as compared to NPC^{-RA} which contained more glial cells. In this context it has been described that a passage number of >20 of a NPC line raises the glial proportion within the neuronal culture (Tang et al., 2013), however, all here described experiments with both of the NPC lines (NPC^{-RA} and NPC^{+RA}) were performed during passages #10–20 of the NPCs. Therefore, we conclude from our observations and the transcriptomic analysis that the RA treatment during early neurulation has a beneficial effect on the neurodevelopment since more neurons survive during terminal differentiation stages in the NPC^{+RA} line compared to the NPC^{-RA} line. Since terminal differentiation is induced by bFGF withdrawal it should be mentioned that RA and FGF have an interesting regulatory relationship in morphogenesis (Casci, 2008; White et al., 2007). In this study it was suggested that removal of FGF may effectively up-regulate RA signalling. This, however, should not play a role in our study

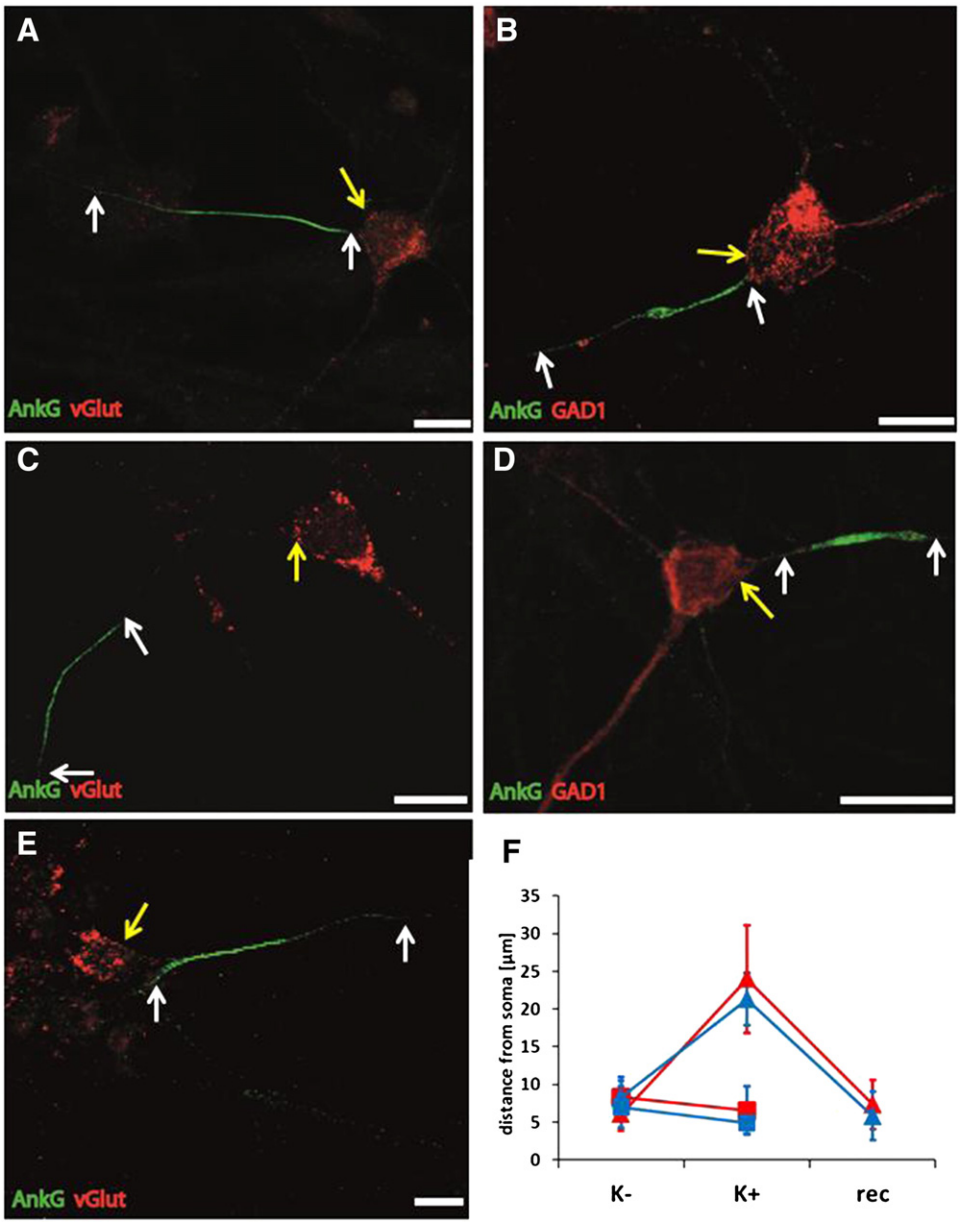

Figure 4 Early RA treatment has no influence on AIS movement. For visualization of the AIS the protein AnkyrinG was stained by immunofluorescence. As marker proteins vGlut1 was used for glutamatergic cells (A, C, E) and GAD1 for GABAergic cells (B, D). Cells were either untreated (A + B) or chronically depolarized with 15 mM K^+ (C + D), and fixed with 4% PFA afterwards. For recovery experiments cells were kept in 15 mM K^+ for 2 days and for further 2 days in neuronal differentiation medium and fixed afterwards (E). Representative Figures A, B, C, D, and E were obtained with the NPC^{-RA} line. In Figures A–E white arrows point to the beginning and ending of the AIS region (AnkyrinG staining) and a yellow arrow indicates the corresponding cell soma, respectively. Scale bars 10 µm. (F) Quantification of distal AIS shifts. The AIS moves significantly in glutamatergic neurons derived from NPC^{-RA} and NPC^{+RA} (▲, ▲; $p < 0.0001$, student's t-test). This shift is reversible upon removal of KCl for 2 days. No KCl-induced shift was observed in GABAergic neurons derived from NPC^{-RA} and NPC^{+RA}, respectively (■, ■). At least 40 cells were analyzed per data point from at least three individual experiments per cell line.

since we apply RA during EB formation in the absence of bFGF, and apply bFGF only in later phases.

One hypothesis for the observed effects of early RA treatment could be the fact that RA acts on retinoic acid responsive elements (RAREs) which are among others located at the promoter of the pluripotency transcription factor Oct4 (Pikarsky et al., 1994). Thereby Oct4 gets down-regulated and in combination with the triple SMAD inhibition with the neural inductors noggin, dorsomorphin and SB431542, the cells are directed to a neural fate. Thus, early RA treatment may positively impact on this development. In a comparable approach RA treatment had been shown to alter the oligosaccharide cell surface antigen expression of terato-carcinoma NCCIT cells during their neuronal differentiation

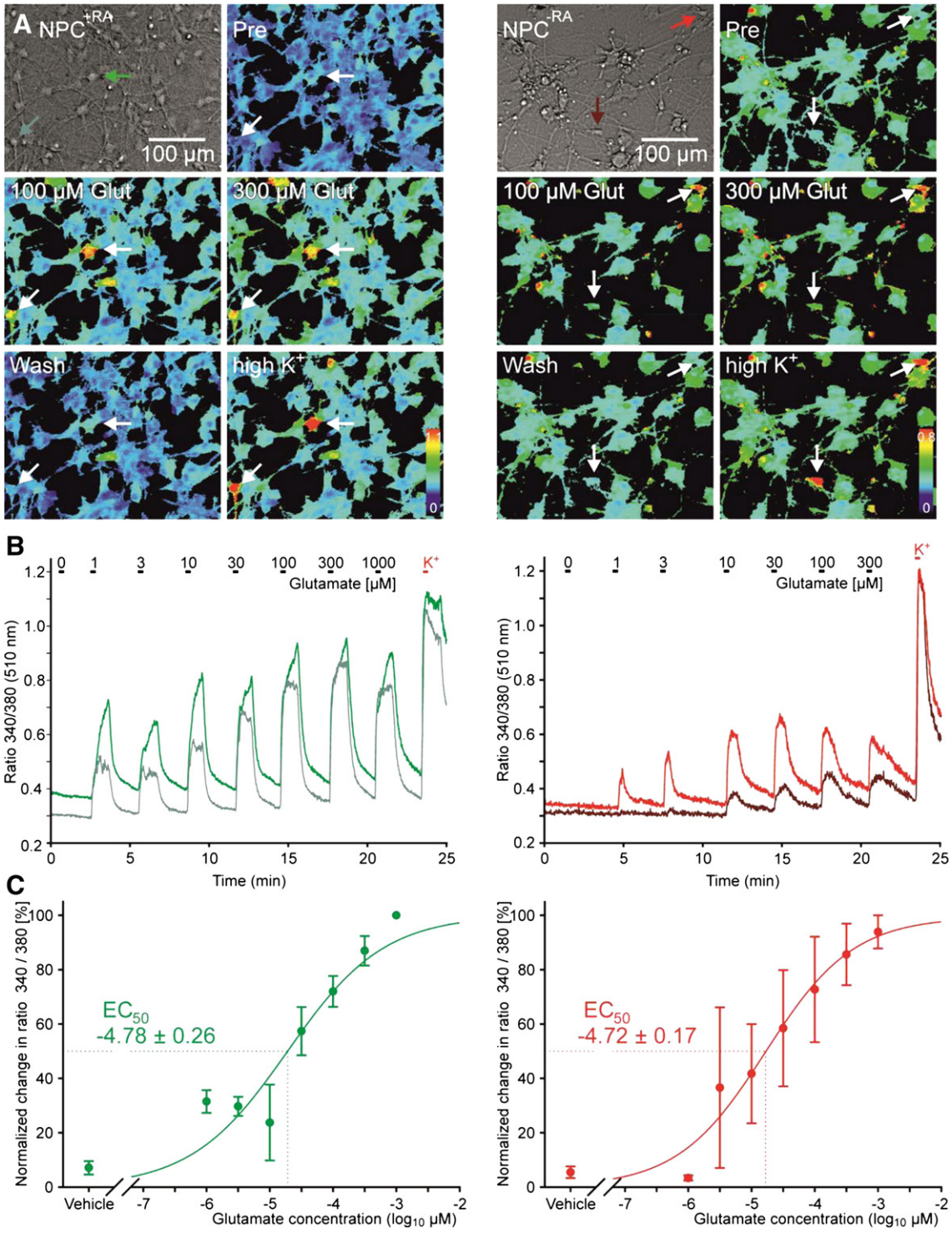

Figure 5 Calcium imaging reveals similar glutamate sensitivity of NPC^{-RA} and NPC^{+RA} derived neurons. FURA-2 ratiometric calcium transient imaging was performed in hiPSC-derived neuronal cultures at least at day 50 of terminal differentiation. (A) False colour pictures of representative experiments displaying cells before glutamate application (Pre), challenged with different concentrations of glutamate, and after depolarization using 140 mM extracellular potassium solution. (B) Calcium changes over time of the two representative cells of NPC^{+RA} (left)/NPC^{-RA} (right) marked with arrows in (A), respectively. Glutamate concentrations are indicated at the top. (C) Mean dose response curves for NPC lines (mean ± SEM). EC_{50} values are indicated by dashed lines. Shown graphs are representative for one experiment (n = 3 per cell line). Left columns display NPC^{+RA}, on the right NPC^{-RA}.

and also to increase the expression of the decorin core protein which is known to promote axonal growth (Gasimli et al., 2013; Minor et al., 2008). Whether comparable mechanisms may underlie the development of longer axons in the RA treated cell line NPC^{+RA} remains to be investigated.

Furthermore, we assessed the excitability of the differentiated neurons by quantifying glutamate-induced calcium influx and by activity-dependent AIS movements. The latter is an immunofluorescence-based method to visualize activity-dependent neuronal plasticity in developing neurons: With this respect Grubb and Burrone had shown that chronic mild depolarization of glutamatergic neurons from rat hippocampal cultures induced a distal shift of the AIS from the cell soma (Grubb and Burrone, 2010). This movement was reversible and not seen in GABAergic neurons. Comparably to Grubb and Burrone also we observed in our study a KCl-induced, reversible distal shift of the AIS only in glutamatergic neurons with the magnitude of the analyzed shift corresponding to the measurements performed in rat hippocampal neurons (Grubb and Burrone, 2010). Hereby, the distance of the AIS movement did not significantly differ in NPC^{-RA} and NPC^{+RA} derived neurons, respectively.

Quantification of glutamate-evoked calcium transients did not reveal any differences between NPC^{-RA} and NPC^{+RA} derived neurons. In both lines, glutamate dose-dependently evoked Ca^{2+} influx with an EC_{50} value of 15–20 μM. Because Ca^{2+} measurements were performed in the presence of Mg^{2+} and in the absence of the NMDA-coactivator glycine and glutamate-induced Ca^{2+} fluxes were completely blocked by 10 μM CNQX but not affected by 20 μM APV we assume that Ca^{2+} influxes measured in our hiPSC-derived neurons were mediated by glutamate receptors of the AMPA-, and not the NMDA subtype.

In summary, our data provide evidence that preconditioning with RA during the neural induction phase of NPC generation favours the relation of neuronal versus glial cells and impacts on neurite lengths, especially axonal length during terminal differentiation of hiPSCs. On the other hand, RA treatment does not influence functional parameters of terminally differentiated neurons such as transmitter induced excitability or neuronal plasticity estimated by activity-dependent AIS movement. Therefore, early RA treatment may be favourable for the neuronal differentiation of hiPSCs resulting in a neuronal population with a predominantly glutamatergic phenotype.

Abbreviations

hiPSC	human induced pluripotent stem cell
AIS	axon initial segment
RA	retinoic acid
NPC	neuronal precursor cell
EB	embryoid body
AnkG	ankyrinG
SHH	sonic hedgehog
CNTF	ciliary neurotrophic factor
RARE	retinoic acid responsive element

Disclosures

The funders had no role in study design or preparation of the manuscript. The authors have no conflicts of interest to declare.

Acknowledgements

We thank Isabell Moskal and Gina Tillmann for their excellent technical assistance and Dr. Thorsten Lau for his critical reading of the manuscript. This work was supported by the Deutsche Forschungsgemeinschaft (SFB636 to A.M-L., J.U.) and by the Foundation Roger de Spoelberch (A.M-L.).

Appendix A. Supplementary data

Supplementary data to this article can be found online at http://dx.doi.org/10.1016/j.scr.2015.04.007.

References

Allodi, I., Hedlund, E., 2014. Directed midbrain and spinal cord neurogenesis from pluripotent stem cells to model development and disease in a dish. Front. Neurosci. 8 (109), 1–18.

Amoroso, M.W., Croft, G.F., Williams, D.J., O'Keeffe, S., Carrasco, M.A., Davis, A.R., et al., 2013. Accelerated high-yield generation of limb-innervating motor neurons from human stem cells. J. Neurosci. 33 (2), 574–586.

Bain, G., Ray, W.J., Yao, M., Gottlieb, D.I., 1996. Retinoic acid promotes neural and represses mesodermal gene expression in mouse embryonic stem cells in culture. Biochem. Biophys. Res. Commun. 223 (3), 691–694.

Bibel, M., Richter, J., Schrenk, K., Tucker, K.L., Staiger, V., Korte, M., et al., 2004. Differentiation of mouse embryonic stem cells into a defined neuronal lineage. Nat. Neurosci. 7 (9), 1003–1009.

Brennand, K.J., Simone, A., Jou, J., Gelboin-Burkhart, C., Tran, N., Sangar, S., et al., 2011. Modelling schizophrenia using human induced pluripotent stem cells. Nature 473 (7346), 221–225.

Casci, T., 2008. Developmental biology: retinoic acid passes the morphogen test. Nat. Rev. Genet. 9 (1), 7-7.

Chambers, D., Wilson, L., Alfonsi, F., Hunter, E., Saxena, U., Blanc, E., et al., 2009a. Rhombomere-specific analysis reveals the repertoire of genetic cues expressed across the developing hindbrain. Neural Dev. 4 (1), 6.

Chambers, S.M., Fasano, C.A., Papapetrou, E.P., Tomishima, M., Sadelain, M., Studer, L., 2009b. Highly efficient neural conversion of human ES and iPS cells by dual inhibition of SMAD signaling. Nat. Biotechnol. 27, 275–280.

Chen, Y., Reese, D.H., 2011. The retinol signaling pathway in mouse pluripotent P19 cells. J. Cell. Biochem. 112 (10), 2865–2872.

Dotti, C., Sullivan, C., Banker, G., 1988. The establishment of polarity by hippocampal neurons in culture. J. Neurosci. 8 (4), 1454–1468.

Falk, A., Koch, P., Kesavan, J., Takashima, Y., Ladewig, J., Alexander, M., et al., 2012. Capture of neuroepithelial-like stem cells from pluripotent stem cells provides a versatile system for in vitro production of human neurons. PLoS ONE 7 (1), e29597.

Gasimli, L., Stansfield, H., Nairn, A., Liu, H., Paluh, J., Yang, B., et al., 2013. Structural remodeling of proteoglycans upon retinoic acid-induced differentiation of NCCIT cells. Glycoconj. J. 30 (5), 497–510.

Greffrath, W., Kirschstein, T., Nawrath, H., Treede, R.D., 2001. Changes in cytosolic calcium in response to noxious heat and their relationship to vanilloid receptors in rat dorsal root ganglion neurons. Neuroscience 104 (2), 539–550.

Grubb, M.S., Burrone, J., 2010. Activity-dependent relocation of the axon initial segment fine-tunes neuronal excitability. Nature 465 (7301), 1070–1074.

Grynkiewicz, G., Poenie, M., Tsien, R.Y., 1985. A new generation of Ca^{2+} indicators with greatly improved fluorescence properties. J. Biol. Chem. 260 (6), 3440–3450.

Gudas, L.J., Wagner, J.A., 2011. Retinoids regulate stem cell differentiation. J. Cell. Physiol. 226 (2), 322–330.

Hansen, D., Rubenstein, J., Kriegstein, A., 2011. Deriving excitatory neurons of the neocortex from pluripotent stem cells. Neuron 70 (4), 645–660.

Hebert, J.M., Fishell, G., 2008. The genetics of early telencephalon patterning: some assembly required. Nat. Rev. Neurosci. 9 (9), 678–685.

Horschitz, S., Meyer-Lindenberg, A., Schloss, P., 2010. Generation of neuronal cells from human peripheral blood mononuclear cells. Neuroreport 21 (3), 185–190.

Kim, J.-E., O'Sullivan, M.L., Sanchez, C.A., Hwang, M., Israel, M.A., Brennand, K., et al., 2011. Investigating synapse formation and function using human pluripotent stem cell-derived neurons. Proc. Natl. Acad. Sci. U. S. A. 108 (7), 3005–3010.

Kim, D.-S., Ross, P.J., Zaslavsky, K., Ellis, J., 2014. Optimizing neuronal differentiation from induced pluripotent stem cells to model ASD. Front. Cell. Neurosci. 8 (109), 1–16.

Lippmann, E.S., Estevez-Silva, M.C., Ashton, R.S., 2014. Defined human pluripotent stem cell culture enables highly efficient neuroepithelium derivation without small molecule inhibitors. Stem Cells 32 (4), 1032–1042.

Liu, H., Zhang, S.-C., 2011. Specification of neuronal and glial subtypes from human pluripotent stem cells. Cell. Mol. Life Sci. 68 (24), 3995–4008.

Maden, M., 2001. Role and distribution of retinoic acid during CNS development. Int. Rev. Cytol. 209, 1–77.

Maden, M., 2007. Retinoic acid in the development, regeneration and maintenance of the nervous system. Nat. Rev. Neurosci. 8 (10), 755–765.

Maherali, N., Ahfeldt, T., Rigamonti, A., Utikal, J., Cowan, C., Hochedlinger, K., 2008. A high-efficiency system for the generation and study of human induced pluripotent stem cells. Cell Stem Cell 3 (3), 340–345.

Marchetto, M.C.N., Carromeu, C., Acab, A., Yu, D., Yeo, G.W., Mu, Y., et al., 2010. A model for neural development and treatment of Rett syndrome using human induced pluripotent stem cells. Cell 143 (4), 527–539.

McCormick, D.A., Prince, D.A., 1987. Post-natal development of electrophysiological properties of rat cerebral cortical pyramidal neurones. J. Physiol. 393 (1), 743–762.

Minor, K., Tang, X., Kahrilas, G., Archibald, S.J., Davies, J.E., Davies, S.J., 2008. Decorin promotes robust axon growth on inhibitory CSPGs and myelin via a direct effect on neurons. Neurobiol. Dis. 32 (1), 88–95.

Napoli, J.L., 2012. Physiological insights into all-trans-retinoic acid biosynthesis. Biochim. Biophys. Acta 1821 (1), 152–167.

Orsolits, B., Borsy, A., Madarász, E., Mészáros, Z., Kőhidi, T., Markó, K., et al., 2013. Retinoid machinery in distinct neural stem cell populations with different retinoid responsiveness. Stem Cells Dev. 22 (20), 2777–2793.

Påhlman, S., Ruusala, A.-I., Abrahamsson, L., Mattsson, M.E.K., Esscher, T., 1984. Retinoic acid-induced differentiation of cultured human neuroblastoma cells: a comparison with phorbolester-induced differentiation. Cell Differ. 14 (2), 135–144.

Paschaki, M., Schneider, C., Rhinn, M., Thibault-Carpentier, C., Dembélé, D., Niederreither, K., et al., 2013. Transcriptomic analysis of murine embryos lacking endogenous retinoic acid signaling. PLoS ONE 8 (4), e62274.

Pikarsky, E., Sharir, H., Ben-Shushan, E., Bergman, Y., 1994. Retinoic acid represses Oct-3/4 gene expression through several retinoic acid-responsive elements located in the promoter–enhancer region. Mol. Cell. Biol. 14 (2), 1026–1038.

Prè, D., Nestor, M.W., Sproul, A.A., Jacob, S., Koppensteiner, P., Chinchalongporn, V., et al., 2014. A time course analysis of the electrophysiological properties of neurons differentiated from human induced pluripotent stem cells (iPSCs). PLoS ONE 9 (7), e103418.

Rochette-Egly, C., 2014. Retinoic acid signaling and mouse embryonic stem cell differentiation: cross talk between genomic and non-genomic effects of RA. Biochim. Biophys. Acta Mol. Cell Biol. Lipids 1851 (1), 66–75.

Sartore, R.C., Campos, P.B., Trujillo, C.A., Ramalho, B.L., Negraes, P.D., Paulsen, B.S., et al., 2011. Retinoic acid-treated pluripotent stem cells undergoing neurogenesis present increased aneuploidy and micronuclei formation. PLoS ONE 6 (6), e20667.

Shi, Y., Kirwan, P., Smith, J., Robinson, H.P.C., Livesey, F.J., 2012. Human cerebral cortex development from pluripotent stem cells to functional excitatory synapses. Nat. Neurosci. 15 (3), 477–486.

Siegenthaler, J.A., Ashique, A.M., Zarbalis, K., Patterson, K.P., Hecht, J.H., Kane, M.A., et al., 2009. Retinoic acid from the meninges regulates cortical neuron generation. Cell 139 (3), 597–609.

Somers, A., Jean, J.-C., Sommer, C.A., Omari, A., Ford, C.C., Mills, J.A., et al., 2010. Generation of transgene-free lung disease-specific human induced pluripotent stem cells using a single excisable lentiviral stem cell cassette. Stem Cells 28 (10), 1728–1740.

Stern, C.D., 2001. Initial patterning of the central nervous system: how many organizers? Nat. Rev. Neurosci. 2 (2), 92–98.

Takahashi, K., Yamanaka, S., 2006. Induction of pluripotent stem cells from mouse embryonic and adult fibroblast cultures by defined factors. Cell 126 (4), 663–676.

Tang, X., Zhou, L., Wagner, A.M., Marchetto, M.C.N., Muotri, A.R., Gage, F.H., et al., 2013. Astroglial cells regulate the developmental timeline of human neurons differentiated from induced pluripotent stem cells. Stem Cell Res. 11 (2), 743–757.

Tonge, P.D., Andrews, P.W., 2010. Retinoic acid directs neuronal differentiation of human pluripotent stem cell lines in a non-cell-autonomous manner. Differentiation 80 (1), 20–30.

Uchida, N., Buck, D.W., He, D., Reitsma, M.J., Masek, M., Phan, T.V., et al., 2000. Direct isolation of human central nervous system stem cells. Proc. Natl. Acad. Sci. U. S. A. 97 (26), 14720–14725.

Ungrin, M.D., Joshi, C., Nica, A., Bauwens, C., Zandstra, P.W., 2008. Reproducible, ultra high-throughput formation of multicellular organization from single cell suspension-derived human embryonic stem cell aggregates. PLoS ONE 3 (2), e1565.

Verpelli, C., Carlessi, L., Bechi, G., Fusar Poli, E., Orellana, D., Heise, C., et al., 2013. Comparative neuronal differentiation of self-renewing neural progenitor cell lines obtained from human induced pluripotent stem cells. Front. Cell. Neurosci. 7.

White, R.J., Nie, Q., Lander, A.D., Schilling, T.F., 2007. Complex regulation of *cyp26a1* creates a robust retinoic acid gradient in the zebrafish embryo. PLoS Biol. 5 (11), e304.

Zeng, H., Guo, M., Martins-Taylor, K., Wang, X., Zhang, Z., Park, J.W., et al., 2010. Specification of region-specific neurons including forebrain glutamatergic neurons from human induced pluripotent stem cells. PLoS ONE 5 (7), e11853.

Zhang, S.-C., Wernig, M., Duncan, I.D., Brüstle, O., Thomson, J.A., 2001. In vitro differentiation of transplantable neural precursors from human embryonic stem cells. Nat. Biotechnol. 19 (12), 1129.